INTERNATIONAL JOURNAL OF HYDROGEN ENERGY 35 (2010) 4668–4675

Available at www.sciencedirect.com

journal homepage: www.elsevier.com/locate/he

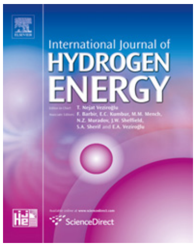

Effect of excess oxygen in plasma reforming of diesel fuel

Dae Hoon Lee, Kwan-Tae Kim, Min Suk Cha, Young-Hoon Song[*]

Green Environmental System Research Department, Korea Institute of Machinery & Materials, 171 Jang-dong, Yusong-gu, Daejeon 305-343, Republic of Korea

ARTICLE INFO

Article history:
Received 15 October 2009
Received in revised form
18 February 2010
Accepted 19 February 2010
Available online 26 March 2010

Keywords:
Plasma
Reforming
Diesel
Oxygen to carbon ratio

ABSTRACT

This study investigated the plasma reforming process for diesel focusing on the relative ratio of oxygen to fuel. Excess O_2 in the partial oxidation process is known to increase the combustion portion, resulting in a decreased yield of H_2 and CO. However, in this parametric investigation, there was no apparent decrease in the H_2 and CO selectivity. Adding O_2 did not increase the portion of combustion in the overall reaction. Rather, an excess O_2 supply from partial oxidation stoichiometry resulted in an increase in CO_2 selectivity without a reduction in CO selectivity. Heavy hydrocarbon species were identified as a source of CO_2 in excess O_2 conditions due to preferential oxidative cracking. The additional oxidation of C_1–C_4 species by excess O_2 provided a minor contribution to CO_2. Excess O_2 affects soot generation characteristics by suppressing the agglomeration of soot particles, resulting in smaller particle generation. However, the oxidation of soot particles does not provide a major contribution to increasing the CO_2 selectivity. The results show that in a real reforming process, controlling the O_2 supply does not have a strong effect on the process selectivity of hydrogen.

© 2010 Professor T. Nejat Veziroglu. Published by Elsevier Ltd. All rights reserved.

1. Introduction

Emerging environmental issues have produced tight regulations to reduce CO_2 emissions in the energy and transportation fields [1]. Moreover, the expectation for petroleum oil to run out has created a demand in technology for alternative fuels and renewable energy. In accordance with this trend, the notation for H_2 and CO_2 economics is introduced. In this period of transition from HC-based economics to H_2-based economics, synthesis gas has emerged as a bridging step of development [2,3]; as it is mainly composed of H_2 and CO, synthesis gas can be obtained from existing fuels. Synthesis gas has been used as a raw material in C_1 chemistry for decades, but it is now being used in new applications: a reducing agent in de-NO_x systems, alternative fuel, the connecting stage in processing synthetic diesel from biomass and waste, and many other environmentally friendly applications [4,5].

Clean diesel engines that compete with hybrid engines in fuel efficiency exhaust a lesser amount of CO_2, but reducing the amount of NO_x and particulate matter (PM) has become an issue. PM can be reduced through facilities such as diesel particulate filters (DPFs), and NOx can be reduced into N_2 through de-NOx facilities such as LNT and SCR. Here, the technical issue is the selection of the reducing agent and reduction catalysts [5,6].

With the abovementioned background, this paper introduces a plasma reformer that converts diesel fuel into synthesis gas. Previous researches on diesel reforming mainly adopted the catalytic reforming process [7,8]. And the plasma reforming process has been recently tried. Both catalytic and plasma reforming process have pros and cons and plasma has

---

[*] *Corresponding author*. Tel.: +82 42 868 7302; fax: +82 42 868 7284.
E-mail addresses: dhlee@kimm.re.kr (D.H. Lee), ktkim@kimm.re.kr (K.-T. Kim), mscha@kimm.re.kr (M.S. Cha), yhsong@kimm.re.kr (Y.-H. Song).

0360-3199/$ – see front matter © 2010 Professor T. Nejat Veziroglu. Published by Elsevier Ltd. All rights reserved.
doi:10.1016/j.ijhydene.2010.02.091

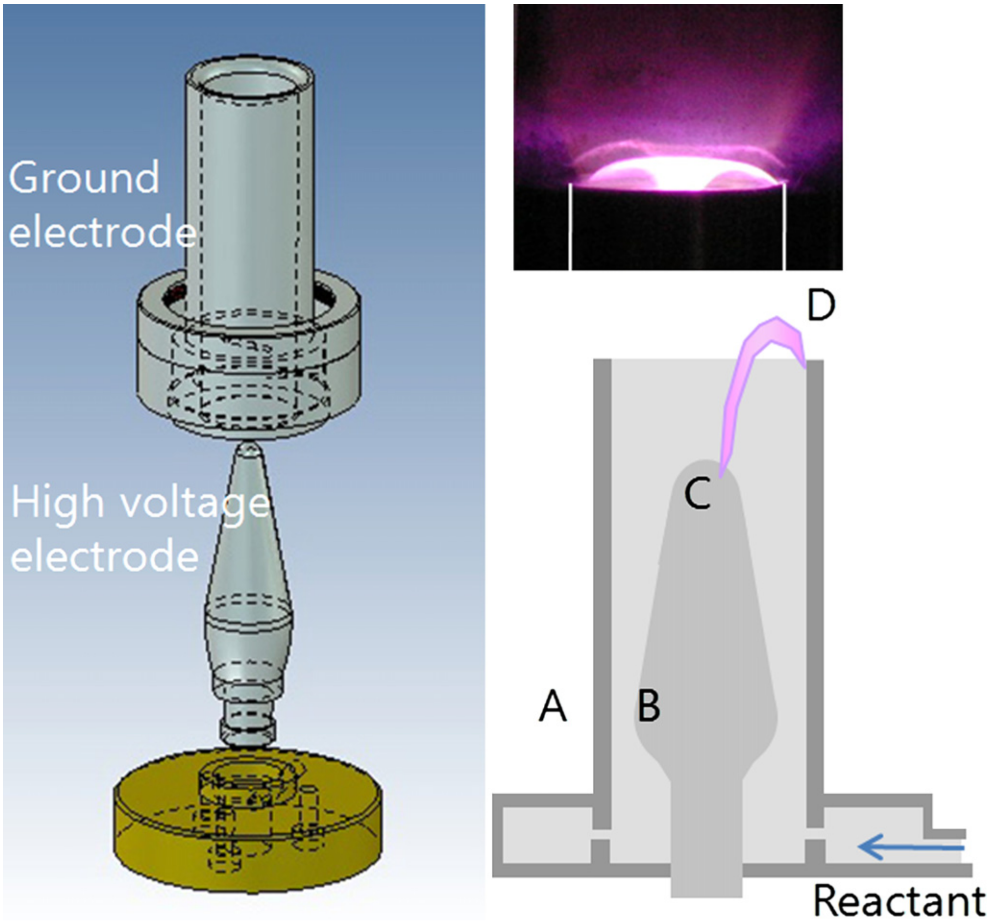

Fig. 1 – Schematic of rotating arc and generation of expanded arc with rotational motion.

advantages in fast startup and tolerance to soot deposition. There have been reports on diverse plasma types for reforming [9–11]. Most of the studies on plasma reforming have used gas-phase hydrocarbon fuels such as methane and propane. In their paper, Petipas et al. [11] reviewed a diverse number of plasma sources used in the reforming process.

Although the plasma reforming process consumes additional electric power, it has many beneficial aspects: a fast startup, ease of control, coking insensitivity, and a rather small scale of reactor, which provides hope for its prospective use in on-board applications. In on-board applications, power consumption should be within the amount available from a battery. Therefore, the development of plasma reformer that aims for on-board applications should maximize the hydrogen production while minimizing the power consumption. To optimize the reforming process, the parameters of the reforming process should be analyzed in terms of hydrogen yield and process efficiency. Among the various parameters of the reforming process, the O_2/C ratio, or the molar ratio of oxygen to fuel carbon, is known to play an important role, as it has strong correlation to the heat release and reaction path [9]. This study investigated the role of O_2/C in the plasma reforming process for diesel; it verified that, in contrast to current knowledge [12], an increase in O_2 does not lead to an increase in the combustion process rate. During verification, analyses of the behavior of C_1–C_4 species and the characteristics of soot generation were carried out.

2. Experiment

2.1. Rotating arc

The plasma reformer used in this study is based on a rotating-arc reactor [9]. As shown in Fig. 1, the rotating-arc reactor is composed of a cylindrical ground electrode and a conical high-voltage electrode within. The reactant is introduced from the holes located at the bottom of the reactor. The influx of reactant flow is directed tangentially to generate a swirling flow within the reactor. Through this swirling reactant flow, the discharging arc is convected downstream with an expanded length. The discharge process takes place through the following steps. First, the discharge ignites at the minimum gap point between electrodes (A–B). The arc string then moves downstream to touch the end of the electrode (C–D). And after that, it blow out and the arc string is re-ignited at A–B, and the procedure is repeated. However, under some controlled conditions, the arc does not detach but becomes anchored at the edge of both electrodes (C–D) and rotates without re-ignition at A–B, as shown in the figure (right upper

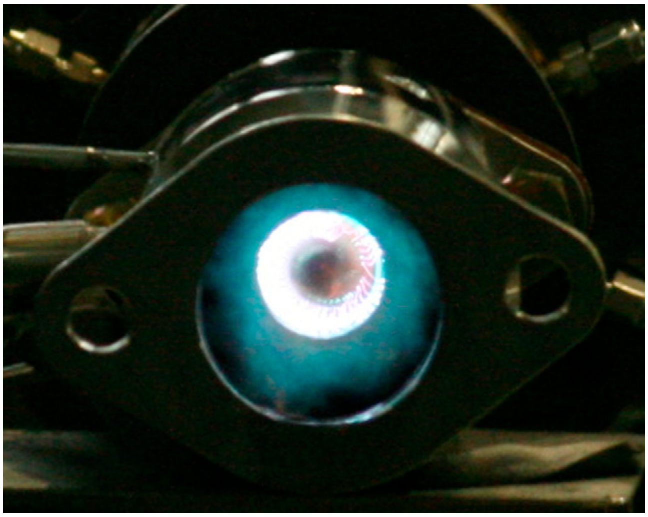

Fig. 2 – Blue flame observed in plasma reforming process of liquid-phase diesel.

part). A higher degree of ionization for the gas between the electrodes makes the path C–D more conductive than A–B; this is why the arc continuously stays at C–D. Normally, electric field between A and B is higher than that of C and D. However, reforming process, hosted from C–D region to downstream, much elevate the temperature between C and D resulting in locally lowered density and increased reactive species. Moreover, rotational flow within the reactor has effect of heat confinement making the region C–D more conductive. All of these effects are synergetic in elevation of degree of ionization. This change in mode maximizes the effective reaction volume and is crucial for hydrogen production with less energy [9].

All of the abovementioned characteristics provide an advantageous environment for fuel vaporization, gaseous fuel and oxidant mixing, and gas-phase reforming; these are essential steps for diesel fuel reforming. Liquid-phase fuel is injected through the holes located close to the tip of the high-voltage electrode that functions like a nozzle. Fuel is atomized by the nozzle, and atomizing airflow. Fast vaporization and mixing then take place due to the high-temperature environment within the reactor and the discharging airflow. As a result, under controlled conditions, even the blue flame that is usually observed in the gas-phase reaction can be observed, as shown in Fig. 2. The hole for fuel injection has a diameter of 0.6–1.0 mm. Most of the air required for the reaction is provided through a connecting plenum located circumferentially outside the cylindrical reactor. The plenum has multiple holes that guide air into the reactor tangentially to create a swirling flow inside the reactor. The sum of the flow rates of the reaction and atomizing airflows gives the amount of air required for the partial oxidation reaction.

The experimental apparatus used was the same as that used in a previous study by the authors for methane reforming [9]. The product of the reforming process was analyzed by GC, H_2 by TCD (Carboxen1010) and HC by FID (HP-AL/KCL). Product gas was sampled after moisture was removed by chiller and provided to column by Tedlar gas sampling bag (CEL®). GC was calibrated before analysis with standard gases with the composition of 1) $H_2/CO/N_2/CO_2$ (3.00/5.08/88.86/3.06), 2) $H_2/CO/N_2/CO_2$ (11.80/20.00/56.10/12.10), 3) $CH_4/C_2H_6/C_2H_4/C_3H_8/n\text{-}C_4H_{10}/C_2H_2/C_3H_6/i\text{-}C_4H_{10}/N_2$ (0.5050/0.0501/0.5110/0.0502/0.0504/0.5260/0.0490/0.0485/98.6643), 4) $CH_4/C_2H_6/C_2H_4/C_3H_8/n\text{-}C_4H_{10}/C_2H_2/C_3H_6/i\text{-}C_4H_{10}/N_2$ (2.050/0.203/2.070/0.203/0.203/2.130/0.198/0.196/7.253/92.747) and discharge was obtained by an AC power supply with a high-voltage transformer. For the measurement and analysis of particles contained in the reformate gas, a differential mobility analyzer (DMA; TSI 3080) and condensation particle counter (CPC; TSI 3022A) were used.

2.2. *Reaction condition*

The partial oxidation process produces hydrogen from hydrocarbon fuels as described in the following equations. Equation (1) is the primary reforming process of partial oxidation, while Eq. (2) includes the successive shift reaction as well (dry-state reformate condition):

$$C_nH_m + n/2(O_2 + 3.76N_2) \rightarrow nCO + m/2H_2 + 3.76(n/2)N_2 \qquad (1)$$

$$C_nH_m + n(O_2 + 3.76N_2) \rightarrow nCO_2 + m/2H_2 + 3.76nN_2 \qquad (2)$$

Commercial diesel fuel obtained from a gas station was used. Diesel fuel contains so many compositions that it needs to be expressed in terms of a surrogate fuel for analysis. In this study, the surrogate fuel formulation $C_{16}H_{34}$ was used to take the heating value balance into account [13].

With the assumption of the diesel surrogate $C_{16}H_{34}$, the oxygen to carbon ratio (O_2/C) for the reaction stoichiometry of partial oxidation was 0.5 And the tested oxygen to carbon ratios were designed to be 8–14.4. More details on the test conditions are given in Table 1.

3. Results

3.1. *O_2/C as an experimental parameter*

The O_2/C ratio is defined as the molar ratio of oxygen (in air) to carbon number in fuel, and this ratio varies with the fixed total flow rate of the reactant used in the experiment. The specific energy density (SED) is defined as the electric power per unit volume of the reactant and represents the thermal environment of the reaction [9]. Here, SED was obtained on the basis of the assumption of complete fuel vaporization under each

Table 1 – Test condition matrix for fuel flow/airflow rate.

O_2/C	O_2 (lpm)	N_2 (lpm)	Fuel (g/min)	Total flow (lpm)	Power (W)	SED (kJ/L)
0.5	1.9	7.15	2.4	9.29	165	1.07
0.6	1.95	7.32	2.05	9.47	165	1.05
0.7	1.91	7.17	1.72	9.25	165	1.07
0.9	1.90	7.16	1.34	9.20	165	1.08

condition and is listed in Table 1. Because the change in SED was negligible under the tested conditions, the changes in the thermal conditions for the process were regarded as solely due to heat release from a different reaction path due to different O_2/C ratios. The change in heat release affects the conditions for fuel vaporization and mixing. Therefore, the expected effects of changing the O_2/C ratio can be listed as follows: (1) increase in the portion of the combustion process, (2) change in the selectivity of the main product (H_2, CO, CO_2), and (3) change in the amount of hydrocarbon species in the product. The selectivity of the species is given by the equations below:

$$\text{SEL}\ (H_2)(\%) = \frac{1}{17} \times \frac{\text{mole (Produced } H_2)}{\text{mole } (C_{16}H_{34})} \times 100(\%) \tag{3}$$

$$\text{SEL}\ (CO)(\%) = \frac{1}{16} \times \frac{\text{mole (Produced CO)}}{\text{mole } (C_{16}H_{34})} \times 100(\%) \tag{4}$$

$$\text{SEL}\ (CO_2)(\%) = \frac{1}{16} \times \frac{\text{mole (Produced } CO_2)}{\text{mole } (C_{16}H_{34})} \times 100(\%) \tag{5}$$

Strictly speaking, 100% selectivity does not denote complete conversion of the fuel, since the surrogate fuel is not an exact expression of diesel fuel. However, these definitions can give insights to the relative effectiveness of the process.

3.2. *Equilibrium conditions*

Using the thermal equilibrium condition, the effect of the O_2/C ratio on the reforming performance was estimated with the EQUIL module of Chemkin code II [14] with thermodynamic data from Burcat and Ruscic [15]. The results are given in Fig. 3.

The results showed an increase in H_2O and CO_2, while H_2 and CO decreased with increasing O_2/C; this implied a relative increase in the portion of combustion for the overall reaction. The results were re-plotted on a selectivity base. Because the equilibrium calculation was the result of the relative composition or mole fraction of the reaction product and the amount of N_2 remained unchanged during the reaction, the relative production of H_2 and CO to N_2 was re-calculated. The selectivity of selected species by this procedure is given in Fig. 4.

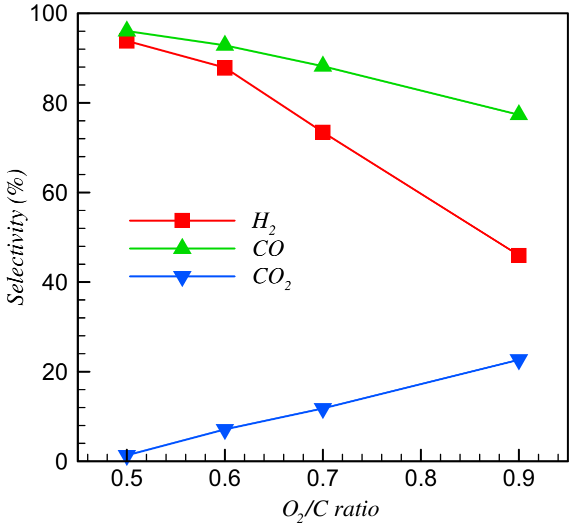

Fig. 4 – Selectivity of H_2/CO/CO_2 derived from equilibrium calculations.

The selectivity of H_2 was more sensitive to the O_2/C ratio than that of CO. The results showed excessively supplied oxygen above reaction stoichiometry of partial oxidation were more prone to oxidize H_2 than CO in a view of equilibrium condition.

3.3. *Reforming conditions and products*

The product of the reforming process using commercial diesel was analyzed. Because the amount of fuel was different for each O_2/C ratio, a comparison based on the selectivity was

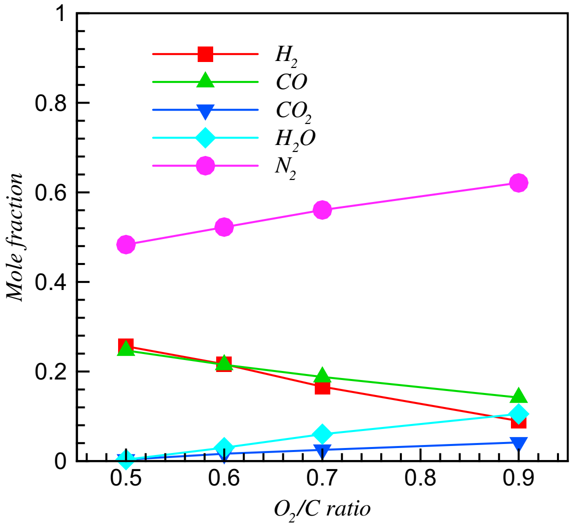

Fig. 3 – Thermal equilibrium composition according to varying O_2/C ratio conditions.

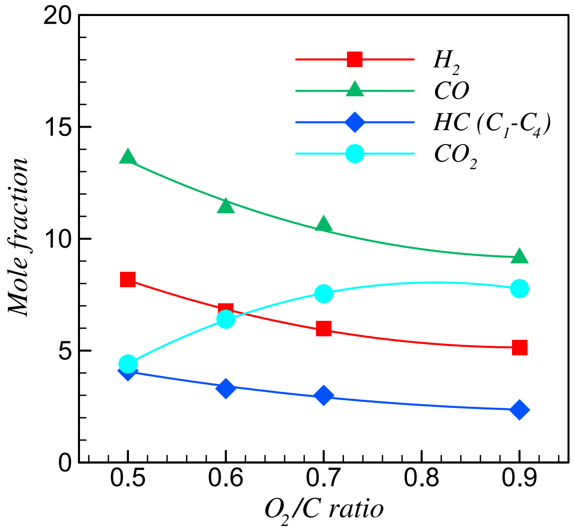

Fig. 5 – Reforming product mole fraction.

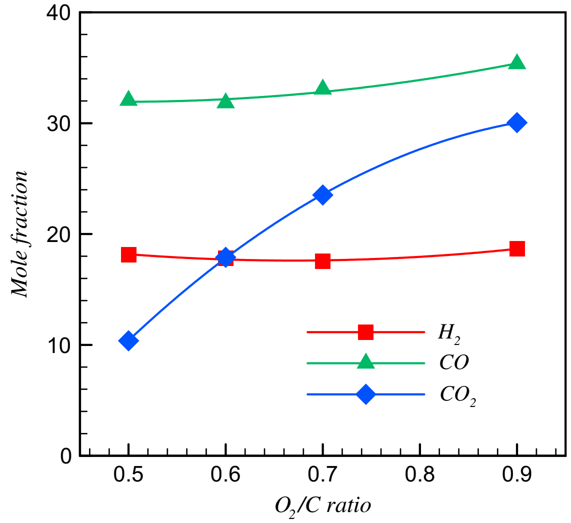

Fig. 6 – Change in selectivity of H_2/CO/CO_2 against O_2/C ratios as derived from obtained data.

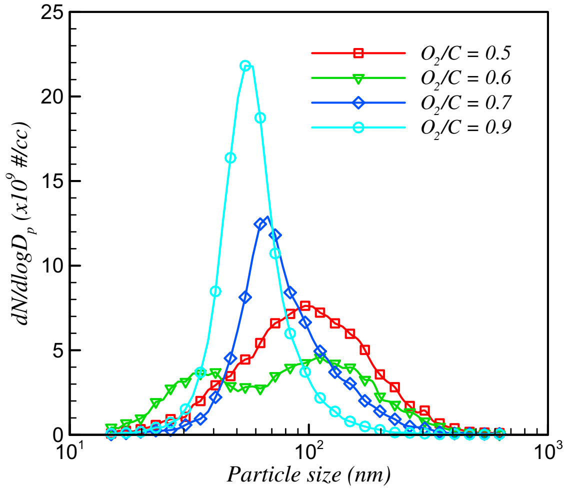

Fig. 8 – Particle size distributions in tested conditions showing characteristics for particle growth and agglomeration according to each O_2/C ratio.

required. Figs. 5 and 6 are the results of mole fraction obtained from the experiment and the derived selectivity for H_2/CO/CO_2. The selectivity of the result was derived with the basis of surrogate fuel of $C_{16}H_{34}$ and within available maximum power of 215 W (140–215 W). If more electric power was supplied and the surrogate was changed, the absolute value of selectivity itself could be much higher. Here, a somewhat different result from that predicted by equilibrium calculation was obtained. The selectivity of H_2 and CO did not show a significant change. However, CO_2 selectivity increased with increasing O_2/C ratio.

Some possible reasons for the selectivity of H_2 and CO not changing considerably are that (1) the plasma-induced process may be affecting the process selectivity by inducing reaction paths other than that of the thermally activated process; or (2) the portion of combustion is not sufficiently high to differentiate the environment of the thermally activated reaction.

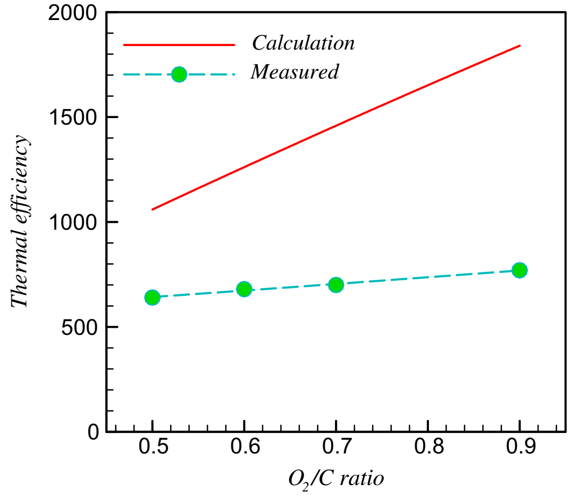

Fig. 7 – Temperature according to O_2/C ratio. Dashed line is for experiment and solid line is for equilibrium calculations.

Because plasma includes chemically active species (CAS) such as electrons, radicals, and excited molecules, some chemistry that was not observed in the thermally activated process might be present. However, for reactions that occur under high-temperature conditions, such as partial oxidation, the relative concentration of CAS (typically 10^{10}–10^{14}/cm^3) is too small to dominate the process. Therefore, the first reason is not sufficient to explain the increase in CO_2 selectivity without a decrease in CO selectivity. A comparison of temperatures can provide an answer to the second problem. Fig. 7 compares the temperature obtained from equilibrium calculations and from the experiment. The point of measurement was the center of the reactor and 7 cm downstream from the conical electrode tip. To insulate the thermocouple from the electric streamer, it was encapsulated in a quartz tube. The encapsulation may have deterred the response and somehow caused an underestimation. However, although the temperature may have been underestimated and the temperature was not a precise representative of the reaction temperature, the increase in temperature with the increasing O_2/C ratio was clearly not sufficiently high to reflect an increased portion of combustion. These results support the conclusion that much of the excess O_2 is not used to increase the portion of oxidation for H_2 and CO and that there are other sources of CO_2 than reformate CO oxidation.

3.4. *Role of additional oxygen*

In the reforming process, possible sources of CO_2 include (1) oxidation of reformate CO, (2) oxidation of carbonaceous species involved in soot generation, (3) oxidation of direct carbon and coke from decomposition and oxidation of lower hydrocarbon ($n \le 4$), and (4) cracking and oxidation of higher hydrocarbons ($n \ge 5$).

Choice (1) is clearly not the answer because the selectivity of CO did not change while the selectivity of CO_2 increased. To figure out the effects of (2), the characteristics of particle generation with varying O_2/C ratios were investigated.

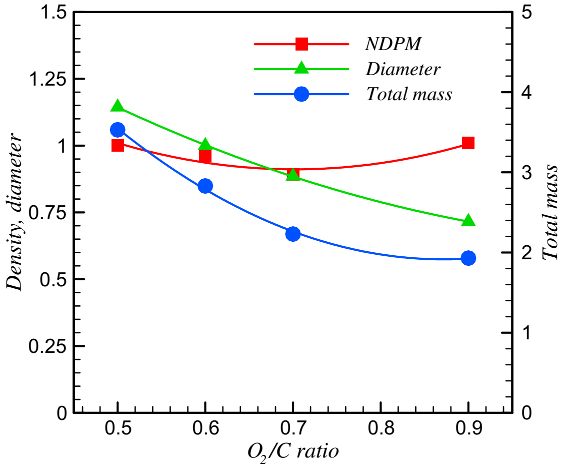

Fig. 9 – NDPM (normalized density per unit mass of reactant particle).

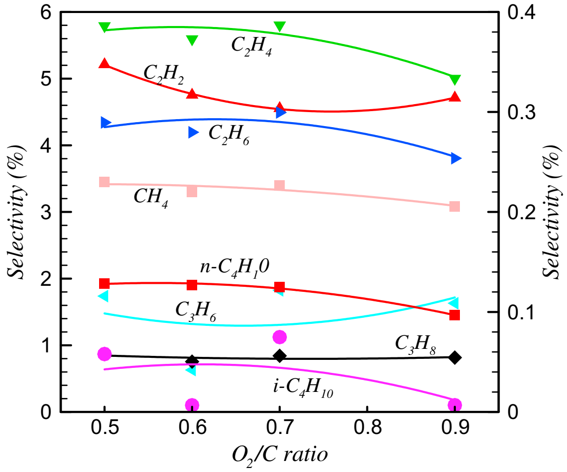

Fig. 10 – Selectivity of C_2 species against O_2/C ratio.

Soot particles that are typically generated in the combustion process follow these steps:

Polycyclic aromatic hydrocarbon (PAH) formation → PAH polymerization → soot inception → agglomeration.

The oxidation of intermediate species in one or multiple steps reduces the particles both in number and size by blocking their inception and agglomeration. Therefore, the amount of CO_2 from the oxidation of intermediate species of soot can be estimated by measuring the particle number and size using differential mobility analyzer and condensation particle counter. In the experiment, the amount of fuel was different for each O_2/C ratio, and the amount of fuel itself can affect the agglomeration characteristics. Therefore, the total number and particle generation by unit mass of fuel was also compared. The particle size distribution for each O_2/C ratio is given in Fig. 8.

When the O_2/C ratio was 0.5, agglomerated particles typically around 100 nm in size were observed. As the O_2/C ratio increased, the distribution became bimodal ($O_2/C = 0.6$), as an intermediate stage of agglomeration was shown from the primary particle (first peak about 20 nm) to the agglomerated particle (second peak about 100 nm). Further increases in the O_2/C ratio resulted in somewhat different behavior. As the O_2/C increased, the bimodal state disappeared; further agglomeration of the particles disappeared, but a shift in the peak for the primary particle was observed. (The normal peak for the primary particle is around 20 nm.) The shift in the peak implied sintering and the growth of primary particles without agglomeration, which is common at high temperatures and when the particles are of low density[16]. In terms of temperature (Fig. 7), there was no real change in temperature due to increased O_2/C (about 100 °C); the temperature did not seem to have a meaningful effect on the prevention of agglomeration.

Table 2 – HC species measured by GC.

C number	Species
C_1	CH_4
C_2	C_2H_2, C_2H_4, C_2H_6
C_3	C_3H_6, C_3H_8
C_4	i-C_4H_{10}, n-C_4H_{10}

Further information on the particle mean diameter, total mass, and particle generation per unit mass of fuel is given in Fig. 9. (NDPM: the density per unit mass was normalized to the value of O_2/C ratio as 0.5; i.e., the NDPM of $O_2/C = 0.5$ is one.)

Although the NDPM did not experience much change, the density and diameter showed a monotonic decrease. This means that the number of particles generated by a unit mass of fuel was not affected by varying O_2/C ratios; therefore, the excess oxygen only affects the agglomeration process. There was not much oxidation of carbonaceous species by the addition of O_2, and thus did not contribute to the increase in CO_2 selectivity.

Process (3), or the oxidation of direct carbon and coke from decomposition and oxidation of lower hydrocarbon, was also investigated. Generally, in partial oxidation of hydrocarbons, the coke-free condition requires a temperature above 1000 °C [17] therefore, the carbon and carbonaceous particulate generation is not negligible in the tested condition of this study. Direct carbon generation during the reforming process typically proceeds, though not necessarily always, in the following sequence [18]:

C_nH_m → Olefins → Polymers → Coke → Amorphous carbon → Graphitic carbon

Direct carbon is rather small in size and difficult to measure with a particle analyzer. In addition, elemental carbon is known to be generated mainly from the decomposition of C_1–C_4 species [16]. Therefore, the generation and oxidation of direct carbon and coke can be inferred from the selectivity change of these hydrocarbon species. Table 2 lists the species considered in this study.

The selectivity of the above HC species is given in Fig. 10. Except for the C_3 species, most of the species have slightly negative correlations with the O_2/C ratio; as the oxygen is

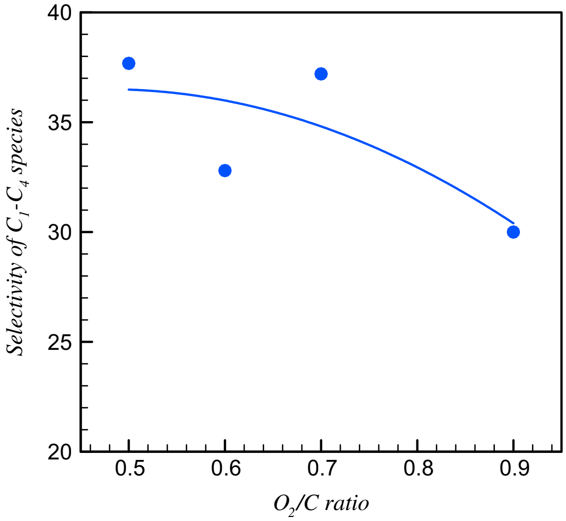

Fig. 11 – Sum of carbon numbers in C_1–C_4 species against O_2/C ratio. Here, the sum of the carbon numbers may be the index for CO_2 selectivity.

added, decomposition and oxidation of the HC species take place. This may be the source for the increased selectivity of CO_2. Based on the measured selectivity, the contribution of HC species to the increase in CO_2 selectivity was estimated. As the higher HC species contribute more to CO_2 generation, the weighted sum of selectivity was compared for each O_2/C ratio. The expression of the weighted sum is defined in the following equation. A smaller weighted sum (W.S) results in a bigger contribution to the increase in selectivity of CO_2.

$$W.S(O_2/C) = \sum_{n=1}^{4} S(O_2/C)_{nm} \times n \qquad (6)$$

where Snm is the selectivity of species C_nH_m.

The sum is plotted against O_2/C ratio in Fig. 11. An increase in O_2/C clearly results in a decrease in selectivity of HC species. However, although the reduction is clear, it is not enough to compensate for the amount of increase in CO_2 selectivity for the increment of CO_2 due to oxidation of reduced carbons in HC species (C_1–C_4) only accounts for one-third or less of the amount.

Consequently, as a result of estimating the possible sources of CO_2 (candidate processes (1)–(3)), most of the CO_2 was inferred to come from oxidative cracking of heavy hydrocarbon species, which is why additional oxygen seems to be preferentially involved in the cracking, oxidation, and dehydrogenation of heavy hydrocarbon species. This is also why when there is excess O_2, no visible decrease in H_2 and CO was observed in contrast to theoretical analysis, which expects that the addition of excess O_2 increases the portion of complete oxidation or combustion [12]. Detailed analysis of each species of heavy hydrocarbon is not available as that was not in the scope of this study. Further kinetic study on oxidative cracking of heavy hydrocarbons may reveal the mechanism for excess O_2 consumption.

Table 3 – SIED according to O_2/C condition.

O_2/C	0.5	0.6	0.7	0.9
SED (kJ/L)	1.07	1.05	1.07	1.08
SIED (kJ/L_{H_2})	13.37	16.36	19.51	23.99

The effect of excess O_2, in terms of process efficiency for hydrogen production was also estimated by defining the specific input energy density (SIED, kJ/L_{H_2}) as the amount of electric power supplied for the production of a unit volume of H_2. The results are tabulated in Table 3.

Here, SIED is a parameter in viewpoint of only product. How much of electric power is required to produce target product and it does not concern the process itself. So we need another parameter for the efficiency of the process itself or thermal efficiency. Typically thermal efficiency can be defined as in Eq. (7) [19]

$$\eta = \frac{(N_{H_2} + N_{CO}) \cdot LHV_{H_2}}{N_{fuel} \cdot LHV_{fuel} + Q_{in}} \qquad (7)$$

The changes in thermal efficiency by varying O_2/C ratio condition are given in Fig. 12. (Test condition in Fig. 12 is not for a maximum efficiency condition, it only shows parametric effect of O_2/C ratio in efficiency.)

Thermal efficiency does not show much difference along with O_2/C ratio that means the selectivity of hydrogen does not have strong correlation with O_2/C ratio within tested condition. However, as the O_2/C ratio increases, thermal efficiency approaches that of equilibrium condition. That is why as the O_2/C ratio increases, relatively high-temperature environment is provided that is favorable for H_2 production. Input power was 9–16% of LHV of fuel. To verify O_2/C effect on thermal efficiency, the effect of relative plasma power should be isolated. So, the effect of O_2/C ratio on thermal efficiency and SIED are compared on the basis of the same {plasma power/fuel heating value} base.

As is shown in Table 4, O_2/C ratio does not affect much on thermal efficiency. Confirming aforementioned results that excess O_2 preferentially affects oxidation process of

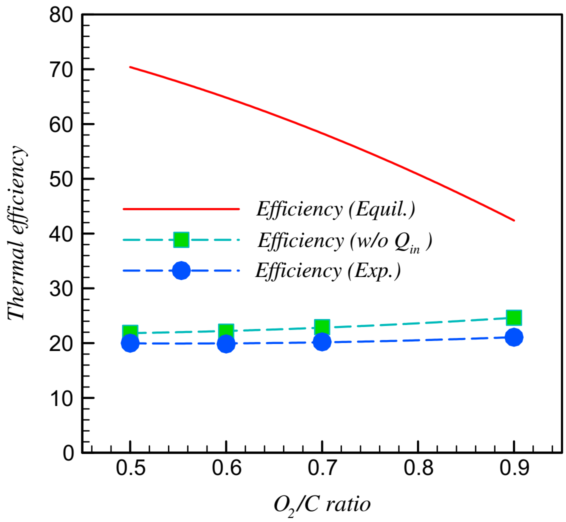

Fig. 12 – Thermal efficiency of the reforming process for equilibrium condition (solid line), experimental result calculated without plasma power in denominator (rectangle) experimental result with plasma power (circle).

Table 4 – Thermal efficiency and SIED in constant power to heating value condition.

O_2/C	0.5	0.7	1.0
Thermal efficiency (%)	20.32	20.15	20.29
SIED (kJ/L_{H_2})	11.53	15.27	16.03

carbonaceous species instead of H_2 generation process. However, SIED shows difference that is why SIED only focuses process efficiency of H_2 production.

4. Conclusion

The diesel reforming process was investigated with a particular focus on the effect of the O_2/C ratio. The composition of the reforming product was compared with the equilibrium condition. The addition of O_2 was expected to increase the portion of the combustion process, but the temperature and selectivity of H_2 and CO showed that the increase in the combustion portion was less than what is expected from equilibrium conditions. Only the selectivity of CO_2 increased significantly. Possible sources of CO_2 in the reforming process include (1) oxidation of reformate CO, (2) oxidation of carbonaceous species involved in soot generation, (3) oxidation of direct carbon and coke from decomposition and oxidation of lower hydrocarbon ($n \leq 4$), and (4) cracking and oxidation of higher hydrocarbons ($n \geq 5$). Of these choices, the contribution of processes (1)–(3) to an increase in CO_2 selectivity was shown to be minor. The selectivity of reformate CO does not decrease while the selectivity of CO_2 increases. Analysis on the characteristics of particle generation revealed that excess O_2 has influence on the agglomeration process only and excess O_2 prevents particle agglomeration resulting in decreased particle size and total mass. Tracing the selectivity of C_1–C_4 along with O_2/C showed that decomposition and oxidation of direct carbon and coke from these species can produce CO_2, but the amount is at best one-third the increase in CO_2 selectivity. Taking these results into account, it was concluded that heavy HC species with carbon numbers above 5 are mainly responsible for the increase in CO_2 selectivity. Plasma seems to play a specific role in using additional oxygen preferentially for oxidative cracking of heavy hydrocarbon species. Although the selectivity of H_2 does not change with increasing O_2/C, excess O_2 lowers the process efficiency of H_2 generation by introducing oxidation of carbonaceous species.

REFERENCES

[1] Dunn S. Hydrogen futures: toward a sustainable energy system. Int J Hydrogen Energy 2000;27:235–64.

[2] Bobrova L, Zolotarsky I, Sadykov V, Sobyanin V. Hydrogen-rich gas production from gasoline in a short contact time catalytic reactor. Int J Hydrogen Energy 2007; 32:3698–704.

[3] Marban G, Valdes-Solis T. Towards the hydrogen economy? Int J Hydrogen Energy 2007;32:1625–37.

[4] Couhert C, Salvador S, Commandre J-M. Impact of torrefaction on syngas production from wood. Fuel 2009;88: 2286–90.

[5] Smith JA, Bartley GJJ. Stoichiometric operation of a gas engine utilizing synthesis gas and EGR for NO_x control. J Eng Gas Turbine Power 2000;122:617–23.

[6] Sitshebom S, Tsolakis A, Theinnoim K. Promoting hydrocarbon-SCR of NO_x in diesel engine exhaust by hydrogen and fuel reforming. Int J Hydrogen Energy 2009;34: 7842–50.

[7] Kaila RK, Gutierrez A, Outi A, Krause I. Autothermal reforming of simulated and commercial diesel: the performance of zirconia-supported RhPt catalyst in the presence of sulfur. Appl Catal B Environ 2008;84:324–31.

[8] Cheekatamarla PK, Finnerty CM. Synthesis gas production via catalytic partial oxidation reforming of liquid fuels. Int J Hydrogen Energy 2008;33:5012–9.

[9] Lee DH, Kim KT, Cha MS, Song YH. Optimization scheme of a rotating gliding arc reactor for partial oxidation of methane. Proc Comb Inst 2007;31:3343–51.

[10] Horng RF, Lai M-P, Chang Y-P, Yur J-P, Hsieh S-F. Plasma-assisted catalytic reforming of propane and an assessment of its applicability on vehicles. Int J Hydrogen Energy 2009;34: 6280–9.

[11] Petipas G, Rolier J-D, Darmon A, Gonzalez-Aguilar J, Metkemeijer R, Fulcheri L. A comparative study of non-thermal plasma assisted reforming technologies. Int J Hydrogen Energy 2007;32:2848–67.

[12] Lutz AE, Bradshaw RW, Bromberg L, Rabinovich A. Thermodynamic analysis of hydrogen production by partial oxidation reforming. Int J Hydrogen Energy 2004;29:809–16.

[13] Thormann J, Maier L, Pfedfer P, Kunz U, Deutschmann O, Schubert K. Steam reforming of hexadecane over a Rh/CeO_2 catalyst in microchannels: experimental and numerical investigation. Int J Hydrogen Energy 2009;34:5108–20.

[14] Kee RJ, Rupley FM, Miller JA. Chemkin II: a Fortran chemical kinetics package for analysis of gas phase chemical kinetics. Sandia National Laboratories Report 1989; SAND 89-8009B.

[15] Burcat A, Ruscic B. Third millennium ideal gas and condensed phase thermodynamical database for combustion with updates from active thermochemical tables; 2005.

[16] Kittelson DB. Engine and nanoparticles: a review. J Aerosol Sci 1998;29:575–88.

[17] Parmar RD, Kundu A, Karan K. Thermodynamic analysis of diesel reforming process: mapping of carbon formation boundary and representative independent reactions. J Power Sources 2009;194:1007–20.

[18] Shekhawat D, Berry DA, Gardner TH, Spivey JJ. Catalytic reforming of liquid hydrocarbon fuels for fuel cell applications. Catalysis 2006;19:184–253.

[19] Holladay JD, Hu J, King DL, Wang Y. An overview of hydrogen production technologies. Catal Today 2009;139:244–60.